



Originally published as:

Torsvik, T. H., Burke, K., Steinberger, B., Webb, S. J., Ashwal, L. D. (2010): Diamonds sampled by plumes from the core–mantle boundary. - *Nature*, 466, 7304, 352-355

DOI: [10.1038/nature09216](https://doi.org/10.1038/nature09216)

Diamonds Sampled by Plumes From the Core-Mantle Boundary

Trond H. Torsvik^{1,2,3*}, Kevin Burke^{3,4}, Bernhard Steinberger^{5,1,2}, Susan J. Webb³ & Lewis D. Ashwal³

Diamonds were formed under high pressure more than 150 km deep in the Earth's mantle and are brought to the surface mainly by kimberlites. Several thousand kimberlites have been mapped on various scales¹⁻⁴, but it is the distribution of kimberlites in the very old cratons (areas of the continents >2.5 Ga in age and as much as 300 or more km thick⁵) that have evinced most concentrated interest because kimberlites from those areas are the major carriers of economically viable diamond resources. Kimberlites, which are themselves derived from depths of >150 km, provide invaluable information on the composition of the deep sub-continental mantle lithosphere as well as on melting and metasomatic processes at or near the interface with the underlying flowing mantle. Here we use plate reconstructions and tomographic images to show that the edges of the largest heterogeneities in the deepest mantle, stable at least since 200 Ma and probably since 540 Ma, have controlled the eruption of most Phanerozoic kimberlites. Future exploration for kimberlites and their included diamonds should therefore be concentrated in continents with old cratons that in the past overlay these plume generation zones at the core-mantle boundary.

Kimberlites are volatile-rich, potassic ultramafic igneous rocks that vary enormously in composition, mineralogy, texture and isotopic composition, showing evidence of derivation from depleted, enriched and/or fertile mantle sources. The minimum depth of kimberlite generation, based on diamond stability and experimental petrology, is ~150 km^{6,7} but some have suggested far deeper generation depths (400-600 km⁸ or even > 660-1700 km^{9,10}) for kimberlite. Here we put all these results into a wider perspective by demonstrating that most

¹Physics of Geological Processes and Geosciences, University of Oslo, Norway. ²Centre for Geodynamics, NGU, Leiv Eirikssons vei 39, N-7491 Trondheim, Norway. ³School of Geosciences, University of the Witwatersrand, WITS 2050, South Africa. ⁴Department of Geosciences, University of Houston, 312 S&R1 Houston Texas 77204-5007, USA. ⁵Helmholtz Centre Potsdam, German Research Centre for Geosciences, Potsdam, Germany. *To whom correspondence should be addressed: E-Mail: trond.torsvik@ngu.no

kimberlites generated during the past 540 Myr were probably related to plumes that have risen from the two plume generation zones¹¹ (PGZs) at the core mantle boundary (CMB).

Large igneous provinces (LIPs) consist dominantly of basaltic rock erupted relatively rapidly (1-5 Myr) over great areas ($1-10 \times 10^6 \text{ km}^2$)¹². Earlier work has shown that most LIPs of the past 300 Myr, rotated back to their eruption sites, and active deep-plume sourced hotspots at the Earth's surface (Fig. 1), project radially down to lie on narrow stable PGZs on the CMB at the edge of the hot and dense large low shear wave velocity provinces (LLSVPs¹³) of the deep mantle^{11,14-19}, thus demonstrating long-term stability of LLSVPs. The 1% slow velocity contour in the lowermost layer of the SMEAN tomography model²⁰ is a reasonable proxy for the PGZs because most reconstructed LIP eruption sites and steep horizontal gradients in shear-wave anomalies in the SMEAN model fall close to that contour¹⁴. In Figure 1 we show twelve hotspots found by seismic tomography¹⁸ to be sourced by deep plumes. Some other hotspots, which have also been claimed to be sourced from deep plumes using other selection criteria (e.g. Tristan, Reunion, Afar and Hawaii), are not shown on our map, but they too plot close to vertically above the PGZs^{14,16}.

To find out whether kimberlites show an association with PGZs similar to that shown by LIPs and hotspots, we used plate reconstructions^{21,22} to rotate kimberlites that are younger than the initial assembly of Pangea (~320 Ma), to their original eruption sites. We find that eighty percent of kimberlites (1112 of 1395) of the past 320 Myr were erupted when their eruption sites lay above a half-width of 15° on either side of the 1% slow contour of SMEAN in the lowermost mantle beneath Africa (Fig. 1). On average, this dominant part of the kimberlite population plots at a distance of $7 \pm 5^\circ$ from that contour (online supplementary material Table S1). The most anomalous post-320 Ma kimberlites (17%) are in the Slave Province of Canada (Late Cretaceous/Early Tertiary kimberlites²), which was close to a tectonically active continental margin at the times of their eruption.

A remarkable pattern is observed when we plot kimberlites on our series of plate reconstructions. At practically all times, eruption sites plot close to the African PGZ (Fig. 2; S2-S5). For the past 320 Myr, Gondwana with Africa at its heart, has drifted slowly northward over the African PGZ (online supplementary material Figs. S2-S5), and this readily explains the dominance of African (Gondwana) kimberlites in the global record, if, as we suggest, their origin relates to heat from deep plumes. Globally, kimberlite activity peaked between 70 and 120 Ma (Fig. S1), corresponding to the time of formation of some of the most economically viable diamond sources in southern Africa. This time interval overlaps with the most intense known LIP activities in Earth history and a major superchron⁹ of the magnetic

field (~83-120 Ma; Cretaceous Normal Superchron). Almost 25% of all known kimberlites erupted between 80-90 Ma when Africa was moving very slowly (~1 cm/yr) north-eastward with respect to the mantle (Fig. S1).

There are few Phanerozoic kimberlites with ages older than 320 Ma; only about 200 are known between 540 and 320 Ma, and kimberlites were altogether absent from core Gondwana between 370 and 500 Ma — Why? Plate reconstructions provide a possible answer: over this time interval Gondwana was centred on the South Pole and the bulk of the continent was located between, and not over, the two LLSVPs and their marginal PGZs. By the late Devonian (Fig. 3) Gondwana stretched from the South Pole (South Africa) to the equator and kimberlites started to erupt along the equatorial and eastern rim of Gondwana (Australia). At this time kimberlites with economically important diamonds also erupted on the Siberian continent (Yakutsk; 344-376 Ma^{2, 23, 24}). If the stability of LLSVPs and the eruption of LIPs above their margins extend further back than 320 Ma, then we can constrain Gondwana in longitude at 510 Ma and Siberia at 360 Ma by placing the Late Cambrian Kalkarindji LIP in Australia and the Yakutsk LIP above the LLSVP margins (Fig. 4). In this reconstruction, kimberlites in Siberia between 350 and 360 Ma and in Gondwana (Southern Africa) between 500 and 510 Ma (Fig. 3) erupted close to above the African PGZ. Backtracking, we can show that Cambrian kimberlites with economically important diamonds (535-542 Ma²⁵) in Canada fall near the Pacific PGZ, whilst contemporaneous diamond-bearing kimberlites in South Africa erupted above the African PGZ (Fig. 4). Using the Yakutsk and Kalkarindji LIPs to calibrate our global reconstruction in longitude and the principles of plate tectonics, we generated semi-absolute reconstructions for the entire Lower and Middle Palaeozoic, and plot kimberlite distributions from the major kimberlite-bearing continents (Laurentia, Siberia and Gondwana). These reconstructions show that all kimberlites which erupted between 341 and 542 Ma lay, at their times of eruption, above the African (Siberia, Southern Africa) and Pacific (Laurentia, Australia) PGZs (Figs. 3-4). On average those kimberlites plot at a distance of $8 \pm 4^\circ$ from the 1% slow contour of SMEAN, with 93% lying within a half-width of 10° from that contour (Table S1).

Mantle plumes have been argued, using a variety of observations^{9,10,23,26}, to be important in some or all kimberlite eruptions. We have shown elsewhere that LIPs and hotspot volcanoes result from deep-seated mantle plumes that rose from two PGZs^{11,14,15,16}. Here for the first time we show that plumes that have risen from the PGZs at the margins of the sub-African (Figs. 1-2, S2-6) and the Pacific (Figs. 3-4) LLSVPs also to have been involved in kimberlite

eruption. This clustering of kimberlites above LLSVP margins is extremely unlikely to result by chance, and we estimate a probability of 0.1-1% or less.

Kimberlites are only known within continents and ~80% of those erupted during the past 320 Myr formed within a part of a continent that at the time of kimberlite eruption lay close to vertically above a PGZ on the CMB (Fig. 1). The high concentration of economically viable kimberlites in Africa results from old (>2.5 Ga) cratonic parts of the continent lying above a PGZ at various times during the past 320 My. The search for kimberlites and their contained diamonds might be profitably concentrated in areas within the old cratons of continents that overlay a PGZ (Figs. 2, S2-S6). Current limitations in absolute plate reconstructions make it harder to identify such places for times before 320 Ma²⁴. However, if the relationship of LIP and kimberlite eruptions to the PGZs holds before 320 Ma (Figs. 3-4) we can use that information to position continents close to their original longitude long before the assembly of Pangea and probably through the entire Phanerozoic.

It can now be shown that three distinct kinds of igneous bodies represented by (i) at least twelve active hotspot volcanoes¹⁸, (ii) twenty-three LIPs of the past 300 My^{11, 14-16}, and (iii) kimberlites of the past 320 My (this paper) now lie, in the case of the active hotspot volcanoes, or lay, at the time of their eruption in the cases of LIPs and kimberlites, vertically or near vertically above a PGZ on the CMB (Fig. 1). The PGZs can be described as narrow loci of an intermittent or continuous upward flux of hot and buoyant material from the CMB: Lateral flow above the CMB may be deflected upward at the margins of LLSVPs, which are probably chemically distinct^{11,13-17}. This flux appears to be related to the emplacement of LIPs, 'hotspot volcanoes' (of which some, but not all, may lie on tracks that originated in LIPs), and kimberlites.

LIPs and kimberlites have erupted since Archean times. Our results show that most of those rocks have been derived from deep plumes originating at the margins of LLSVPs, but whether the African and Pacific LLSVPs have remained in the same places throughout Earth's history is less certain^{27,16,28}. The stability of LLSVPs in their present locations on the CMB can be demonstrated for LIPs and kimberlites for the past 320 Myr. Most LIPs and kimberlites erupted during the past ~200 Myr, so we can be confident about LLSVP stability since 200 Ma. Explaining those stable LLSVPs and the rising of plumes from their edges requires a new and challenging generation of dynamic mantle models²⁹. We can find a reasonable plate reconstruction with continents placed in longitude such that the two known LIPs and ~200 kimberlites erupted between 540 and 320 Ma fall close to vertically above the present LLSVP margins. This indicates that the near antipodal locations of the two existing

LLSVPs on the equator may have been time-invariant for as much as 540 Myr, and thus seemingly not sensitive to surface plate motions (including the formation of Pangea), as well as mechanically isolated from the convecting mantle.

METHODS SUMMARY (298 words)

We combine reconstructions derived from a hotspot frame for the past 100 Myr and a palaeomagnetic frame back to the initial assembly of Pangea (320 Ma). This is known as the global hybrid frame²¹, which is here corrected for true polar wander²² between 320 and 100 Ma. Before 320 My we used the plume generation zone (PGZ) reconstruction method to calibrate longitudes¹⁶. This method uses the long-term relation between large igneous provinces (LIPs) and the PGZs to estimate longitudes for LIPs and is used here to identify the continents under which the PGZs lay at times of kimberlite eruption. Pre-320 Ma longitudes were calibrated by placing the Yakutsk LIP in Siberia (~360 Ma) and the Kalkarindji LIP in Australia/Gondwana (~510 Ma) over the most likely edges of the African LLSVP¹⁶ (Fig. 4). The palaeolatitude for the Yakutsk (~35°N) and Kalkarindji (~9°N) LIPs are known from palaeomagnetic data from Siberia and Gondwana.

Kimberlite locations were derived from numerous sources (including a recent African compilation³), and include 1395 ‘dated’ kimberlites for the past 320 Myr. Kimberlite age control varies from excellent (e.g. U/Pb dating) to assumed ages based on dated neighbouring kimberlites. Undated or vaguely described ages are not included in our analysis. Each kimberlite site was first rotated to southern African co-ordinates using relative rotation parameters²¹, and subsequently rotated to their correct palaeo-position on the globe (Fig. 1) using the absolute reference frames outlined above. Reconstructed kimberlite eruption sites (symbols in Figs. 1-4 may represent multiple sites) were then draped on the present-day SMEAN anomalies near the core-mantle-boundary (CMB) assuming that the African and the Pacific large low shear wave velocity provinces (LLSVPs) have remained stationary for at least 300 Myr.

Diagrams were produced with GMT (gmt.soest.hawaii.edu), GMAP (www.geodynamics.no), GPlates (www.gplates.org) and SPlates developed for our industry sponsor (Statoil).

Supplementary Information and full methods are available in the online version of the paper at www.nature.com/nature.

- 164 1. Jelsma, H.A. *et al.* Preferential distribution along transcontinental corridors of kimberlites
165 and related rocks of Southern Africa. *S. Afr. J. Geol.* **107**, 301-324 (2004).
- 166 2. Kjarsgaard, B.A. in *Mineral Deposits of Canada: A Synthesis of Major Deposit-Types,*
167 *District Metallogeny, the Evolution of Geological Provinces, and Exploration Methods*
168 (Ed Goodfellow, W.D.) 245-272 (Geol. Assoc. Canada Spec. Public. 5, 2007).
- 169 3. Jelsma, H., Barnett, W., Richards, S. & Lister G. Tectonic setting of kimberlites. *Lithos*
170 **112**, 155-165 (2009).
- 171 4. Heaman, L.M. & Kjarsgaard, B.A. Timing of eastern North American kimberlite
172 magmatism: continental extension of the Great Meteor hotspot track? *Earth Planet. Sci.*
173 *Lett.* **178**, 253-268 (2000).
- 174 5. Jordan, T.H. in *The mantle sample: inclusions in kimberlites and other volcanics* (eds
175 Boyd, F.R. & Meyer, H.O.A.) 1–14 (AGU, Washington, D.C. 1979).
- 176 6. Mitchell, R.H. *Kimberlites: Mineralogy, Geochemistry and Petrology* (Plenum Publishing
177 Company, New York) 442 pp. (1986).
- 178 7. Wyllie, P.J. The origin of kimberlites. *J. Geophys. Res.* **85**, 6902-6910 (1980).
- 179 8. Ringwood, A.E, Kesson, S.E., Hibberson, W. & Ware, N. Origin of kimberlites and
180 related magmas. *Earth Planet. Sci. Lett.* **113**, 521-538 (1992).
- 181 9. Haggerty, S.E. A diamond trilogy: superplumes, supercontinents, and supernovae. *Science*
182 **285**, 851-861 (1999).
- 183 10. Hayman, P.C., Kopylova, M.G. & Kaminsky, F.V. Lower mantle diamonds from Rio
184 Soriso (Juina area, Mato Grosso, Brazil). *Contrib. Mineral. Petrol.* **149**, 430-445 (2005).
- 185 11. Burke, K., Steinberger, B., Torsvik, T.H. & Smethurst, M.A. Plume Generation Zones at
186 the margins of Large Low Shear Velocity Provinces on the Core-Mantle Boundary. *Earth*
187 *Planet. Sci. Lett.* **265**, 49-60 (2008).
- 188 12. Bryan, S. & Ernst, R. Revised definition of Large Igneous Provinces (LIPs). *Earth Sci.*
189 *Rev.* **86**, 175-202 (2008).
- 190 13. Garnero, E.J., Lay, T. & McNamara, A.K. in *Plates, Plumes, and Planetary Processes*
191 (eds Foulger, G.R. & Jurdy, D.M.) 79-109 (Geol. Soc. Am. Spec. Paper 430, 2007).
- 192 14. Torsvik, T. H., Smethurst, M. A., Burke, K. & Steinberger, B. Large igneous provinces
193 generated from the margins of the large low-velocity provinces in the deep mantle.
194 *Geophys. J. Int.* **167**, 1447–1460 (2006).
- 195 15. Torsvik, T.H., Smethurst, M.A., Burke, K. & Steinberger, B. Long term stability in Deep
196 Mantle structure: Evidence from the ca. 300 Ma Skagerrak-Centered Large Igneous
197 Province (the SCLIP). *Earth Planet. Sci. Lett.* **267**, 444-452 (2008).

16. Torsvik, T.H., Steinberger, B., Cocks, L.R.M. & Burke, K. Longitude: Linking Earth's ancient surface to its deep interior. *Earth Planet. Sci. Lett.* **276**, 273-283 (2008).
17. Thorne, M.S., Garnero, E.J. & Grand, S. Geographic correlation between hot spots and deep mantle lateral shear-wave velocity gradients. *Phys. Earth Planet. Inter.* **146**, 47-63 (2004).
18. Montelli, R., Nolet, G., Dahlen, F. & Masters, G. A catalogue of deep mantle plumes: new results from finite-frequency tomography. *Geochem. Geophys. Geosyst.* **7**, Q11007, doi:10.1029/2006GC001248 (2006).
19. Davaille, A., Stutzmann, E., Silveira, G., Besse, J. & Courtillot, V. Convective patterns under the Indo-Atlantic. *Earth Planet. Sci. Lett.* **239**, 233-252 (2005).
20. Becker, T.W. & Boschi, L. A comparison of tomographic and geodynamic mantle models. *Geochem. Geophys. Geosyst.* **3**, 1003, doi:10.1029/2001GC000168 (2002).
21. Torsvik, T.H., Müller, R.D., Van der Voo, R., Steinberger, B. & Gaina, C. Global plate motion frames: Toward a unified model. *Rev. Geophys.* **46**, RG3004, doi:10.1029/2007RG000227 (2008).
22. Steinberger, B. & Torsvik, T.H. Absolute plate motions and true polar wander in the absence of hotspot tracks. *Nature* **452**, 620 (2008).
23. Yakubchuk, A. Diamond deposits of the Siberian craton: Products of post-1200 Ma plume events affecting the lithospheric keel. *Ore Geology Rev.* **35**, 155-163 (2009).
24. Kinny, P.D., Griffin, B.J., Heaman, L.M., Brakhfogel, F.F. & Spetsius, Z.V. Shrimp U-Pb ages of perovskite from Yakutian kimberlites. *Russian Geol. Geophys.* **38**, 97-105 (1997).
25. Heaman, L.M., Kjarsgaard, B.A. & Creaser, R.A. The timing of kimberlite magmatism in North America: implications for global kimberlite genesis and diamond exploration. *Lithos* **71**, 153-184 (2004).
26. Le Roex, A.P., Bell, D.R. & Davis, D. Petrogenesis of Group I Kimberlites from Kimberley, South Africa: Evidence from Bulk-rock Geochemistry. *J. Petrology* **44**, 2261-2286 (2003).
27. Zhong, S., Zhang, N., Li, Z.X. & Roberts, J.H. Supercontinent cycles, true polar wander, and very long-wavelength mantle convection. *Earth Planet. Sci. Lett.* **261**, 551-564 (2007).
28. Li, Z.X. & Zhong, S. Supercontinent–superplume coupling, true polar wander and plume mobility: Plate dominance in whole-mantle tectonics. *Phys. Earth Planet. Inter.* **176**, 143-156 (2009).

29. Tan, E., Leng, W., Zhong, S. & Gurnis, M. On the Fixity of the Thermo-Chemical Piles at the Base of Mantle. *AGU Fall abstract* DI12A-08 (2009).
30. Jaques, A.L. Kimberlite and lamproite diamond pipes. *AGSO J. of Australian Geology and Geophysics* 17, 153-162 (1998).

Acknowledgements

We thank R. Trønnes, S. Haggerty, M. Gurnis and C. Gaina for stimulating comments and discussions, and Scott King and David Evans for constructive reviews. Statoil and the Norwegian Research Council are acknowledged for financial support.

Author Contributions statements

THT and KB developed the conceptual idea for the study, BS developed statistical methods and tests, and SJW and LDA assembled input data. All authors contributed extensively in discussions and writing of the manuscript.

Figure 1 | Reconstructed large igneous provinces (LIPs) and kimberlites for the past 320 Myr with respect to shear-wave anomalies at the base of the mantle. The deep mantle (2800 km on the SMEAN tomography model²⁰) is dominated by two large low shear wave velocity provinces (LLSVPs) beneath Africa and the Pacific. The 1% slow contour (approximation to the plume generation zones; PGZs) is shown as a thick red line. 80% of all reconstructed kimberlite locations (black dots) of the past 320 My erupted near or over the sub-African PGZ). The most “anomalous” kimberlites (17%) are from Canada (white dots). Present day continents are only shown as a background to illustrate the distribution of hotspots classified as of deep plume origin¹⁸ and present day shear-wave anomalies (δV s in percentage), and bear no geographical relationship to reconstructed kimberlites or LIPs.

Figure 2 | Late Jurassic plate reconstruction of continents and kimberlite locations draped on SMEAN. Kimberlite locations with eruption ages between 155-165 Ma were reconstructed to 160 Ma. Reconstructed kimberlite locations are found near the edges of the African LLSVP (near the 1% slow contour), and at the old cratons in North America⁴, NW Africa, South Africa (Kalahari craton¹) and Australia³⁰. The most important cratons for kimberlite eruption since the Carboniferous are shaded in grey.

Figure 3 | Devonian and Cambrian plate reconstructions draped on SMEAN. Kimberlite locations with eruption ages between 350-360 Ma and 500-510 Ma were reconstructed to 355 and 505 Ma; they all fall close to vertically above the SMEAN -1% contours (PGZs).

Figure 4 | Reconstructed Palaeozoic kimberlites from Laurentia (North America, Canada), Siberia and core Gondwana draped on SMEAN.

METHODS (1822 words)

Our methods depend on several factors, including kimberlite age uncertainties and the choice of both plate and tomography models. In addition, plume sources may have been advected in the mantle^{31,32} and a kimberlite eruption site may not mark precisely the site where a plume impinged the base of the lithosphere, but the location of material that may have propagated horizontally within the lithosphere from a plume^{33,34,11,14}. The observation that kimberlites in some cases occur in clusters or lines³ may indicate that their surface distribution is partly

structurally controlled; it is therefore complex to estimate the net effect of these individual uncertainty sources.

We have previously examined nine different shear wave velocity models; they all provide broadly similar characteristics near the CMB so that the choice of tomographic model is not critical to our conclusions^{11,16}, but may lead to slightly different statistical correlations. As an example we compare the 1% slow contour of the SMEAN model with the $\sim 0.96\%$ slow contour in the Castle et al.³⁵ and the $\sim 0.77\%$ slow contour in the Kuo et al.³⁶ D'' models (Fig. S6), which globally, at the CMB, approximately correspond to the 1% slow contour of the SMEAN model¹¹. 25 reconstructed LIPs plot on average at a distance of $8 \pm 9^\circ$ (mean \pm standard deviation) from the SMEAN contour whilst the distances from the CASTLE and KUO contours are reduced to $5 \pm 3^\circ$ and $6 \pm 4^\circ$ (Table S1). In the SMEAN model, 80% of all reconstructed LIPs plots within a 10° half-width centred on the 1% slow contour, increasing to 96% for the CASTLE contour (Table S1, Fig. S7a). The reason that the CASTLE model scores highest is that the CASTLE contour contains two small sub-areas at the CMB that plot near the Siberian Traps (ST in Fig. S6) and the Columbia River Basalt (CB). The CASTLE contour is also continuous further north in the North Atlantic and thus the Iceland hotspot (Fig. 1) also fits better this model. We consider it likely that the Iceland plume is related to a continuation of the Africa LLSVP, and it is possible that the smaller anomaly now underlying the reconstructed Siberia Trap also has been part of the African LLSVP. Different tomography models therefore do matter in a statistical sense, but all three models (and most other models at the CMB^{11,16}) demonstrate that LIPs correlate with the edges of CMB heterogeneities and *never* with their centres.

Kimberlite distribution is also sensitive to the specific tomography model but the $\sim 17\%$ of 'anomalous' Late Cretaceous-Early Tertiary North American kimberlites in the post-320 Ma database ($\sim 12\%$ of the entire Phanerozoic collection) are anomalous in all models. The remaining kimberlites plot at an average distance of $7 \pm 4^\circ$ from the SMEAN contour, $6 \pm 4^\circ$ from the CASTLE contour and $3 \pm 3^\circ$ from the KUO contour (Table S1; 27-314 Myr population). 73% plot within 10° of the SMEAN contour (Fig. S7c). That increases to 85% and 94 % for the CASTLE and KUO contours. For comparison, *in-situ* (i.e. non-reconstructed) kimberlite locations plot at a distance of $19 \pm 12^\circ$ with only 14% inside the 10° band of the SMEAN model — clearly much worse (Fig. S7b). While appreciating the better fit for the CASTLE and KUO models, one also needs to consider that these contours are longer, and hence the area within 10° is larger than for the SMEAN -1% contour. However, the major reason why the KUO model best fits the kimberlite data (Table S1) is that a large

population of 80-90 Ma kimberlites in South Africa (white arrows marked 2 in Fig S6; see also Fig. S4) plot right on top of the 0.77% slow KUO contour, whereas they plot at some distance inside the SMEAN contour.

An absolute plate motion model must account for the distribution of subducted slab material in the mantle through geological time. Such a reference system based on information on subducted slabs identified from seismic tomography and plate kinematic models is still in its infancy but as a plate model sensitivity test we reconstructed kimberlite eruption sites for the past 300 Myr using the subduction reference frame of van der Meer et al.³⁷. Excluding the Late Cretaceous-Early Tertiary North American kimberlites, kimberlites plot at a distance of $9 \pm 4^\circ$ with 65% inside the 10° band for the SMEAN model (Fig. S7c). This is slightly worse but within error of our hybrid plate model.

We have previously given a statistical argument that the coincidence of reconstructed LIPs with the LLSVP margins is extremely unlikely to have resulted from pure chance¹¹, but how likely is it that a kimberlite distribution near the LLSVP edges occurs by chance? Kimberlites only occur in continents and the diamond-bearing kimberlites occur in old >2.5 Ga cratons. Those old cratons make up $\sim 15\%$ of the total area of the continents. In Figure S7d we plot the fraction of cratons that are within 10° of the PGZ as a function of time, based on three tomography models (SMEAN, CASTLE and KUO). This should be equal to the fraction of kimberlites if they were formed randomly on the cratons. For comparison, 62% (dashed red line) of all kimberlites (980 of 1588) are within 10° and 33 % of the surface of the sphere is within 10° based on SMEAN. The percentage of kimberlites (62%) is slightly less than the maximum percentage of cratons ($\sim 70\%$) that are within 10° of the SMEAN slow margin, but importantly, at the times when most of the kimberlites were formed only a much smaller percentage of cratons were within 10° – about the same or even somewhat less than the percentage of the entire surface of the sphere, i.e. what would be expected if the cratons were placed randomly. This shows that the clustering of kimberlites near the 1% slow margin cannot be due to a clustering of cratons near the 1% slow margin. Numbers for the other tomography models CASTLE and KUO are slightly higher but lead to the same conclusion. At the time when most kimberlites formed, cratons were located relative to the 1% slow margin more or less as would be expected from a random distribution, but the kimberlites were *not* formed on the cratons in the way that would be expected in a random distribution. The lighter-coloured dashed lines show that the fraction of kimberlites within 10° of the PGZs becomes somewhat less if we restrict ourselves to more recent times. This may be partly an effect of less freedom in longitude adjustment for more recent times – we have in fact

adjusted longitudes to fit LIPs above PGZs before 320 Ma (Fig. 4). Hence there may be an increasing bias towards also having an increased fraction of kimberlites above PGZs further back in time. Nevertheless, even for the most recent time interval since 130 Ma where longitudes can be constrained by hotspot tracks (although in our reconstruction we switch from hotspot-based to palaeomagnetic reference frame at 100 Ma, but comparison of the two frames shows only a minor difference in longitude between 100 and 130 Ma), the fraction of kimberlites within 10° of PGZs is much higher than the fraction of cratons, so the clustering of kimberlites near PGZs cannot be due to freedom in longitude.

The probability that kimberlites were emplaced randomly is further explored in Figure S8. Calculated probabilities are quite variable, depending on which tomography model is used (different colours), whether we consider the fraction of individual kimberlites within a half width 10° of the PGZs (lines), or the fraction of kimberlite “groups” (filled circles), which time interval is considered and how many independent groups there are. Obviously, results further depend on the half-width and which contour is used to define the PGZs (not shown).

As groups with larger number of kimberlites should presumably be given more weight, we expect that the most appropriate estimate for probability in each case lies somewhere between the filled circles and the line of same colour. We estimate that there are about 43-55 “independent” groups of kimberlites since 542 Ma. As indicated in Figure S7d and Table S1, we expect that with more tight independent constraints on longitude before 130 Ma, and especially before 320 Ma, the fraction of kimberlites within 10° of the PGZs might be slightly (not substantially) less, hence probabilities might be slightly higher than those inferred from the range $N=43-55$. On the other hand, probability estimates from kimberlites since 320 Ma only are rather high, because during that time interval, a large fraction of cratons was already within 10° of the PGZs. However, most kimberlites erupted at times when the fraction of cratons within 10° of the PGZs was much less, hence these estimates are probably too high. Given all this, we expect that the probability for the distribution of kimberlites relative to PGZs being essentially random is about 0.1-1% or less. We emphasize that this estimate considers all kimberlites including the “anomalous” ones from Canada and the large cluster in South Africa, which is reconstructed above the African LLSVP somewhat away from its margin, if the SMEAN 1% slow contour is used. Hence we regard it as highly likely that the distribution of kimberlites is indeed related to the PGZs at the margins of LLSVPs in the lowermost mantle.

It has been suggested that kimberlite eruptions in e.g. North America and Africa occurred during periods of relatively slow continental motion³⁸. In order to test this idea we calculated

the absolute motion of South Africa and North America for the past 320 My (Fig. S1b). Our velocity curves differ from those of England & Houseman³⁸ but we do notice that South Africa has relatively low speeds (1-3.5 cm/yr) during peaks in kimberlite eruption (between 70 and 100 Ma and 110-120 Ma). These lows are also seen for North America but there are two high velocity spikes. The 50-60 Ma spike is associated with ‘anomalous’ kimberlites (Fig. 1, white dots) erupted shortly after the collision of the ribbon continent of the Cordillera with North America, which was a time of tectonic activity in the Canadian Rockies when cracks that fostered decompression melting are likely to have formed in the Slave Province³⁹. Only one lower mantle mineral assemblage has been reported in Cretaceous-Tertiary kimberlites in Canada, but there is abundant majoritic garnet included in diamond⁴⁰⁻⁴¹. A transition zone (410-660 km) activated plume by ‘large scale extension’ seems a reasonable explanation for these ‘anomalous’ kimberlites.

That the reconstructed positions of at least 23 LIPs and now the majority of kimberlites (Fig. 1) all fall near the 1% slow contour is truly remarkable and powerfully demonstrates that the majority of both LIPs and kimberlites are derived from the PGZs near the CMB. These observations are undoubtedly incompatible with passive plate-driven models for LIP genesis⁴², because in such alternative models there should not exist any correlation between surface volcanism and deep mantle heterogeneities; nor is it very likely that upper mantle and crustal processes could affect the polarity pattern of the geodynamo (Fig. S1).

31. Steinberger, B., Sutherland, R. & O'Connell, R.J. Prediction of Emperor-Hawaii seamount locations from a revised model of plate motion and mantle flow. *Nature* **430**, 167-173 (2004).
32. Boschi, L., Becker, T.W. & Steinberger, B. Mantle plumes: dynamic models and seismic images. *Geochem. Geophys. Geosyst.* **8**, Q10006, doi:10.1029/2007GC001733 (2007).
33. Sleep, N.H. Mantle plumes from top to bottom. *Earth Sci. Rev.* **77**, 231-271 (2006).
34. Courtillot, V., Jaupart, C., Manighetti, I., Tapponnier, P. & Besse, J. On causal links between flood basalts and continental breakup. *Earth Planet. Sci. Lett.* **166**, 177-195 (1999).
35. Castle, J.C., Creager, K.C., Winchester, J.P. & van der Hilst R.D. Shear wave speeds at the base of the mantle. *J. Geophys. Res.* **105**, 21543-21558 (2000).
36. Kuo, B.-Y., Garnero, E.J. & Lay, T. Tomographic Inversion of *SSKS* times for shear wave velocity heterogeneity in D": Degree 12 and hybrid models. *J. Geophys. Res.* **105**, 139-157 (2000).

- 415 37. van der Meer, D.G., Spakman, W., van Hinsbergen, D.J.J., Amaru, M.L. & Torsvik, T.H.
 416 Towards absolute plate motions constrained by lower-mantle slab remnants. *Nat. Geosci.*,
 417 **3**, 36-40, doi:10.1038/NGEO708 (2010).
- 418 38. England, P. & Houseman, G. On the geodynamic setting of kimberlite genesis. *Earth*
 419 *Planet. Sci. Lett.* **67**, 109-122 (1984).
- 420 39. Johnston, S. The Cordilleran Ribbon Continent of North America. *Ann. Rev. Earth Planet.*
 421 *Sci.* **36**, 495-530 (2008).
- 422 40. Davies, R., Griffin, W.L., O'Reilly, S.Y. & McCandless, T.E. Inclusions in diamonds
 423 from the K14 and K10 kimberlites, Buffalo Hills, Alberta, Canada: diamond growth in a
 424 plume? *Lithos* **77**, 99-111 (2004).
- 425 41. Stachel, T., Harris, J.W. & Muehlenbachs, K. Sources of carbon in inclusion bearing
 426 diamonds. *Lithos* **112**, 625-637 (2009).
- 427 42. Foulger, G.R. & Jurdy, D.M (eds.), Plates, Plumes, and Planetary Processes (Geol. Soc.
 428 Am. Special Paper **430**, 998 pp., 2007).

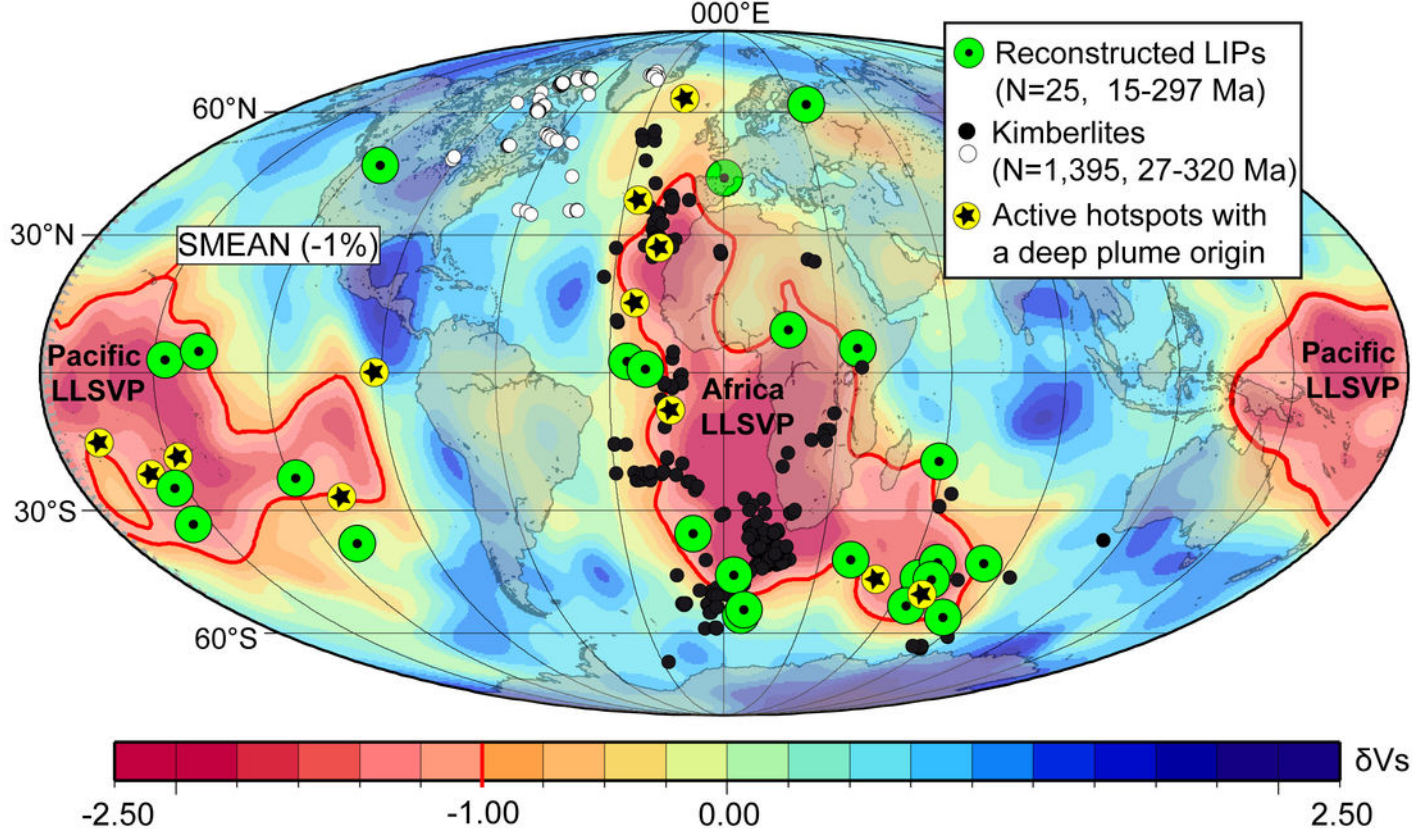


Figure 1 (Torsvik et al. 2010)

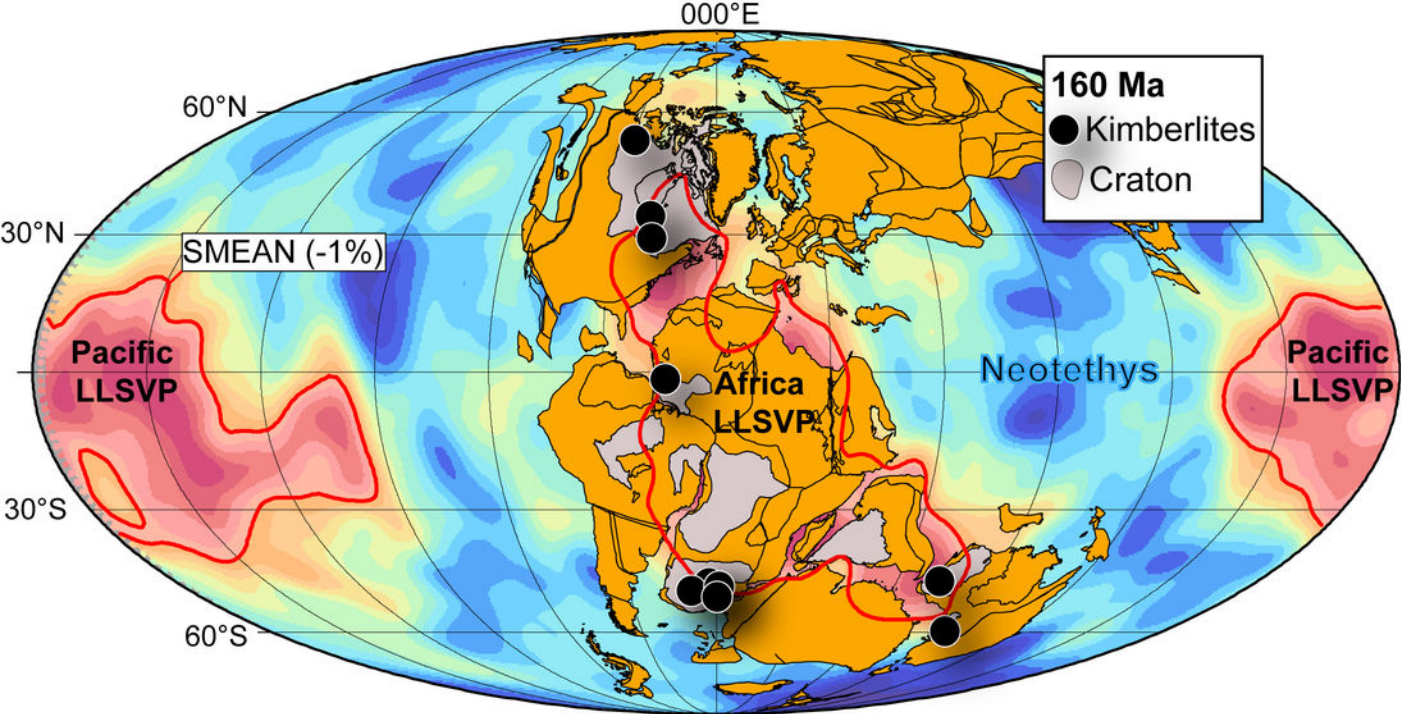
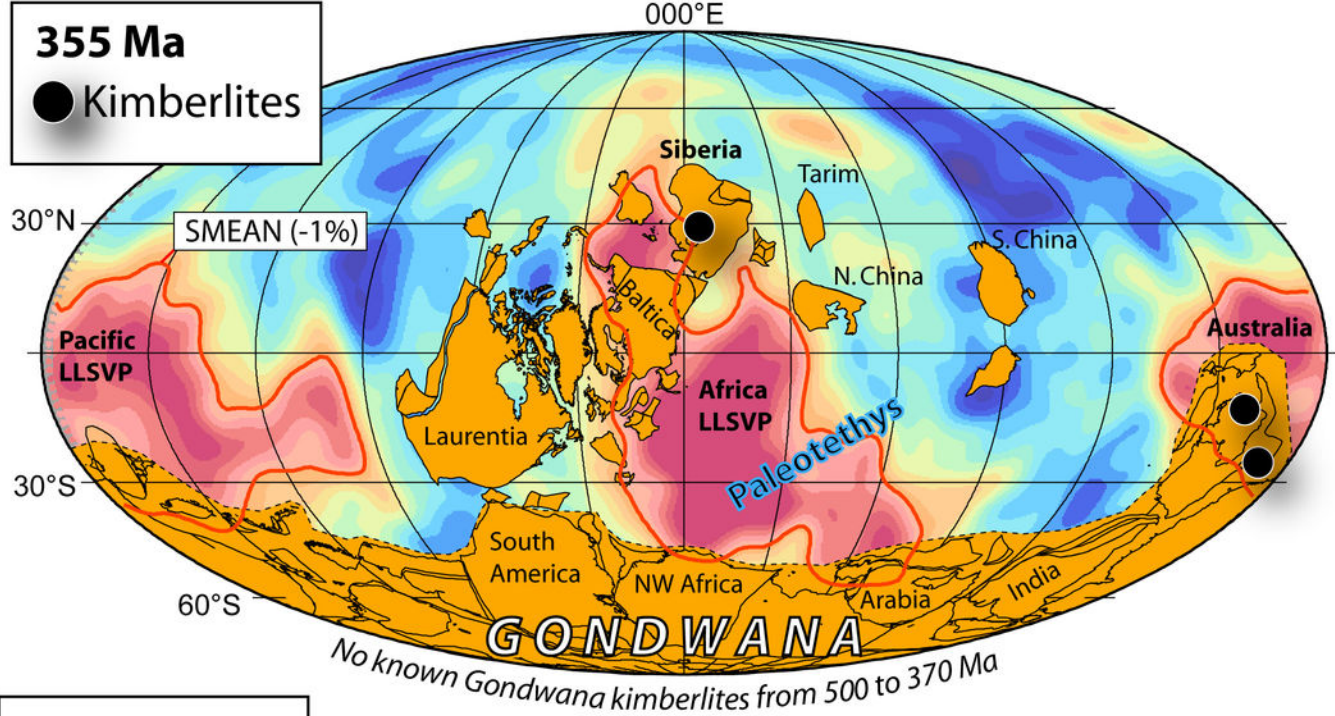


Figure 2 (Torsvik et al. 2010)

355 Ma

● Kimberlites



505 Ma

● Kimberlites

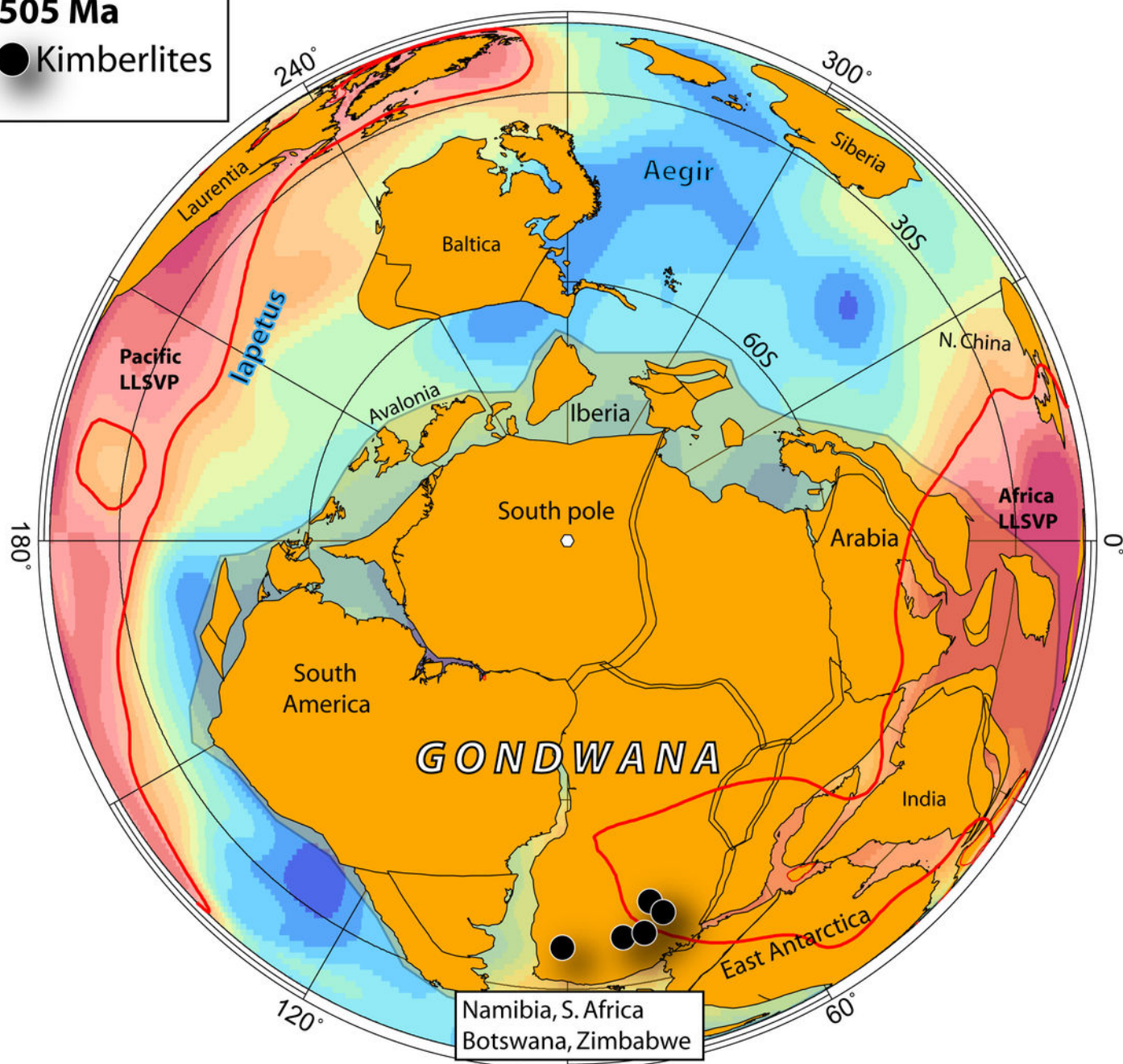


Figure 3 (Torsvik et al. 2020)

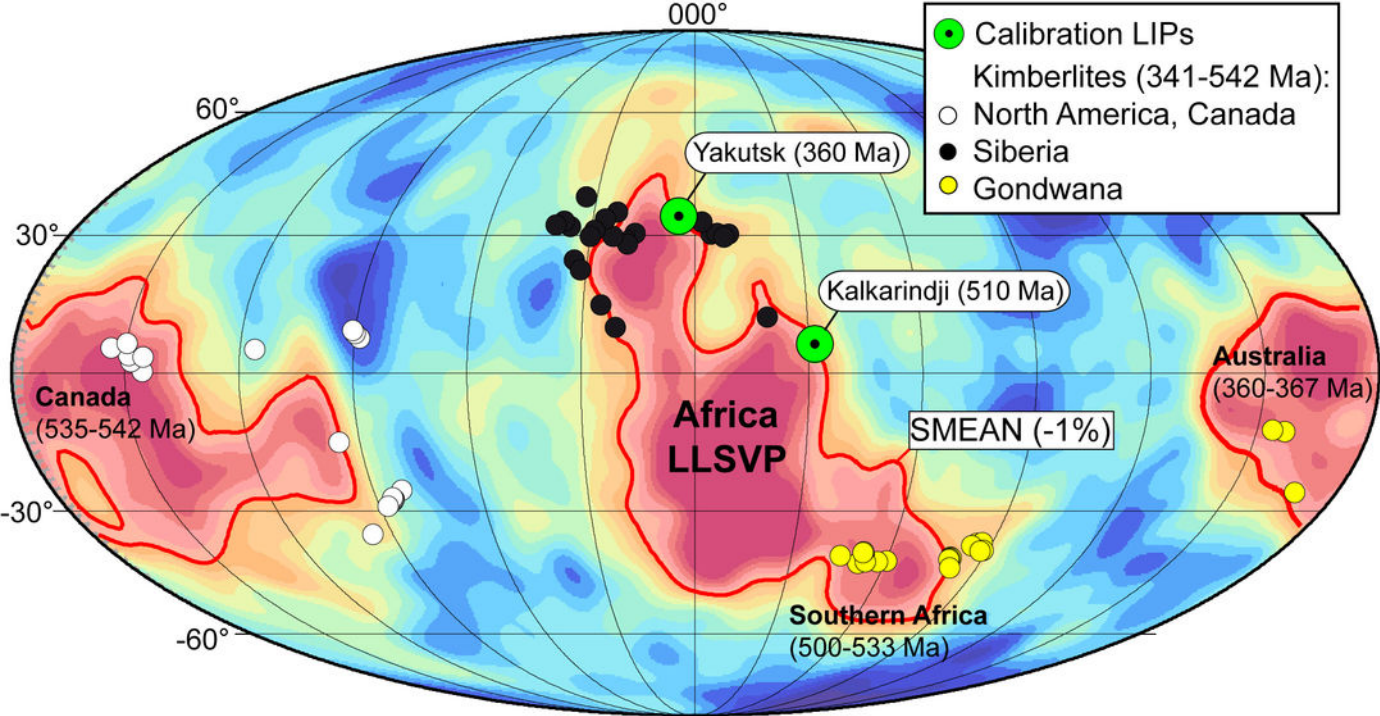


Figure 4 (Torsvik et al. 2010)